

Article

Vulnerability Analysis of Structural Systems under Extreme Flood Events

Fabrizio Greco  and Paolo Lonetti * 

Department of Civil Engineering, University of Calabria, 87036 Rende, CS, Italy

* Correspondence: paolo.lonetti@unical.it; Tel.: +39-0984-496916

Abstract: Vulnerability analyses of coastal or inland bridges in terms of flood actions and structural and fluid flow characteristics are carried out. In particular, a numerical model based on a two-phase fluid flow is implemented for the multiphase fluid system, whereas a three-dimensional formulation based on shell/volume finite elements is adopted for the structure. The governing equations can simulate the interaction between fluids and the structures, by using the Arbitrary Lagrangian–Eulerian (ALE) strategy. The results of the hydrodynamic forces, bridge displacements and dynamic amplification factors (DAFs) show that the existing formulas, available in the literature or in structural design codes, do not accurately predict the maximum design effects. For the investigated cases, the DAFs may vary from 1 to 4.5. The worst scenarios are observed for the upload vertical direction. Finally, the performance of the protection fairing system is investigated. The results show that such devices are able to efficiently reduce the effects of the wave load in terms of the applied hydraulic forces on the structure and bridge deformability, in particular, with 40% more accuracy than the unprotected configuration.

Keywords: fluid–structure interaction; flooding protection strategies; computational fluid dynamics; structural performance



Citation: Greco, F.; Lonetti, P.

Vulnerability Analysis of Structural Systems under Extreme Flood Events.

J. Mar. Sci. Eng. **2022**, *10*, 1121.

<https://doi.org/10.3390/jmse10081121>

Academic Editor: Cristiano Fragassa

Received: 27 June 2022

Accepted: 11 August 2022

Published: 15 August 2022

Publisher's Note: MDPI stays neutral with regard to jurisdictional claims in published maps and institutional affiliations.



Copyright: © 2022 by the authors. Licensee MDPI, Basel, Switzerland. This article is an open access article distributed under the terms and conditions of the Creative Commons Attribution (CC BY) license (<https://creativecommons.org/licenses/by/4.0/>).

1. Introduction

Floods on structures and infrastructure may cause damaging effects and collapse mechanisms, with the loss of human lives and high economic costs, especially in the reconstruction process. In order to reduce such effects, prevention measures should be introduced to reduce the effects of damage on buildings, bridged and other infrastructural systems, using hydraulic constructions or strengthened systems [1]. However, flood events involve complex scenarios, in which an accurate modeling of fluid–structure interaction (FSI) is required to correctly evaluate the magnitude of flood actions on the structure and the structural behavior itself [2]. Bridge response under the action of extreme waves is currently the subject of research in various specialized areas of the research, with the aim of developing tools to improve bridge resistance and quantify damage scenarios. The growth of interest in bridges in coastal areas is mainly due to current concerns about the consequences of climate change and their effects on the intensity of weather hazards. Indeed, such changes in rainfall and storm patterns combined with those in land use have resulted in more frequent and severe storms and floods, and as a result, bridges are experiencing extreme hydrological events more often.

The identification of the damage effects on bridges is performed using several approaches and formulations. Many analyses are based on the direct estimation of flood damage in terms of heuristic or empirical approaches, in which depth–damage curves are determined by statistic data, collected from survey [3] or by means of synthetic vulnerability models based on what-if questions [4]. However, the evaluation of damage effects on structural systems requires a deterministic approach, in which both structural and fluid characteristics should be defined with relative accuracy from both hydrological

or structural points of view [5]. Such analyses are quite important, since the damage assessment at the structural level may influence the results obtained at larger scales, i.e., watershed or basin scales [6]. Therefore, deterministic vulnerability models, able to identify the damage behavior of the structure, are much required for the complete assessment of flood events [7].

From the hydrological point of view, analyses at the macroscale identify the flood characteristics in terms of water depth and velocity, which should be considered as input data to estimate the vulnerability of the structure. However, flood loads depend on other existing factors, such as the scour of the foundation, debris flow, etc. In the literature, most of the models, concerned with identifying the damage caused to buildings, simulate flood actions by means of pseudo-static forces, in which hydrodynamic actions are described by equivalent multiplicative parameters, known in the literature as drag/lift coefficients [6]. In this framework, the hydrostatic nature of the flood actions is considered by means of global coefficients, taken from the literature on the basis of preliminary studies on impact analyses on fixed wall systems. Although the pseudo-static approaches are documented in existing design codes, they rarely consider intrinsic phenomena typically produced by the fluid flow. As a matter of fact, existing studies have shown that at low inlet speeds, the impact is followed by a reflected wave, whose depth is typically larger than the previous one [8]. Moreover, at high speeds, the impact produces the formation of a falling jet and propagating jumps, which affect the height of the wall much more compared to the inlet ones [9]. However, such advanced studies have mostly emphasized the hydraulic aspects of flood events, leaving unanswered questions regarding the effect on structural systems [10,11]. In addition, the fluid actions cannot only be considered as loads applied statically, in view of the presence of the mass of the fluid itself, which can be considered as an additional quantity of inertial terms impacting the structure. As a consequence, the mass of the structure is time dependent and thus its effect should be analyzed in a dynamic framework.

Although many models concerning FSI provide valuable insight on the numerical modeling aspects and force estimation, only a few attempts are made to investigate the vulnerability behavior of the structure under flood actions [12]. The accuracy of the description utilized in the fluid model should also be determine for the structural system, which is typically considered by means of simplified formulations such as fixed or moving wall systems [13–15]. Such modeling strongly differs from the actual deformations of the structure, whose behavior in the case of a wall-based structure should be analyzed using a 3D approach. However, the literature dealing with the analysis of flood effects on structural systems and in particular bridge structures is based on very few studies. In [16], conceptual engineering models quantify the vulnerability of structures, including relevant flood characteristics, such as water depth, flood rise/duration and debris flow, using an equivalent pseudo-static approach. Similarly, a probabilistic modeling based on limit state design, with the purpose of identifying the flood fragility/risk assessment parameters of non-engineered masonry structures, is presented in [17]. Meanwhile, a methodology for calculating the dynamic response of an equivalent single degree of freedom system to the impact of a debris flow is developed in [18]. Finally, a numerical model reproducing FSI on bridge structures is carried out in [19], in which sensitivity studies on the influential parameters of bridge vulnerability are proposed.

The literature mentioned above investigates bridge behavior by considering the interaction between bridges and fluid flows without introducing refined methodologies for the prediction of the structural response. Typically, the structural system is simulated by means of simplified models, which are not able to evaluate the deformability behavior, inertial characteristics and the pressure actions applied by the fluid flow. The present paper proposes a multiscale formulation based on 2D and 3D frameworks. In the former, two-phase field theory is implemented to consider the fluid flow of two immiscible fluids. In the latter, the structural behavior is reproduced by means of 3D finite elements, which provide an accurate definition of bridge characteristics. FSI theory is developed in a cou-

pled two-way approach to consider the mutual effects produced by the bridge motion and pressure distribution on the cross-section boundaries. The present paper can be considered as an extension of previous authors' works [20], in which new results and comparisons are provided. In particular, the main purpose of the present study is to quantify the dynamic amplification effects produced by the fluid motion on the structural system, by means of comparison with existing formulations based on a pseudo-static approach. Moreover, a parametric study in terms of fluid and structural characteristics is developed to evaluate the dynamic amplification factors of the structural system. Finally, the influence of protective systems which can reduce the damage caused to structures is also investigated.

Section 2 presents the multiscale approach with the governing equations of the FSI based on ALE and solid mechanics. In Section 3, the numerical implementation, including the coupling conditions of the multiscale model, is presented, whereas loading configurations and fairing protection systems are described in Section 4. The results expressed in terms of dynamic amplification factors and the effect of fairing systems are proposed in Section 5.

2. Theoretical Formulation

The proposed model is based on a multiscale approach, in which fluid (F) and structure (S) are defined by different unconnected domains (Figure 1). The fluid system is analyzed by means of a 2D approach, in which phase-field theory is implemented to take into account the flood actions produced by the motion of two immiscible fluids, i.e., water (W) and air (A). Moreover, the bridge is modeled using a 3D model, in which a combination of shell/volume elements is utilized to simulate the deformability of the structures. Finally, boundary conditions between each component determine the interaction between fluid and structural systems. The fluid is defined by Navier–Stokes equations for an incompressible fluid, consisting of momentum conservation and continuity equations on the fluid system, i.e., $C^F = C^A \cup C^W$ with $(C^F \times [t_0, t_1])$:

$$\begin{aligned} \rho \frac{d\mathbf{U}}{dt} + \rho (\mathbf{U} \cdot \nabla_{\mathbf{X}} \mathbf{U}) &= \\ &= -\nabla_{\mathbf{X}} \cdot (p \mathbf{I}) + \mu \nabla_{\mathbf{X}} \cdot (\nabla_{\mathbf{X}} \mathbf{U} + \nabla_{\mathbf{X}} \mathbf{U}^T) + \rho \mathbf{g} \\ \nabla_{\mathbf{X}} \mathbf{U} &= 0 \end{aligned} \tag{1}$$

where \mathbf{I} is the identity matrix, \mathbf{U} is the velocity vector, p is pressure function, $[t_0, t_1]$ is the observation period from the initial (t_0) to the final (t_1) time, ρ denotes the density and μ is dynamic viscosity of the fluid. The multiphase fluid flow is described by the phase field variable ϕ on the basis of the advective Cahn–Hilliard equation:

$$\frac{d\phi}{dt} + \mathbf{U} \cdot \nabla_{\mathbf{X}} \phi = \nabla_{\mathbf{X}} \cdot \left(\frac{\gamma \lambda}{\varepsilon^2} \right) \nabla_{\mathbf{X}} \psi \tag{2}$$

where $\psi = -\nabla \cdot \varepsilon^2 \nabla \phi + (\phi^2 - 1)\phi$, λ is the mixing energy density parameter and ε is a capillary width that scales the thickness of the interface. It is worth noting that as far as Reynolds number increases, fluid phase variables are decomposed into average and fluctuating parts on the basis of RANS approach [21].

In order to handle moving boundaries based on the fluid motion, the moving mesh technique is implemented. Such an approach is based on the Arbitrary Lagrangian–Eulerian (ALE) formulation, in which positional variables from fixed to the current configurations are described on the basis of a mapping function ζ [22], as follows:

$$\mathbf{X} = \zeta \left(\mathbf{r}, t \right) \tag{3}$$

where \underline{r} and \underline{X} are the referential and material point coordinates [23]. Consistently with the ALE approach, the equations of the fluid flow are expressed in terms of the referential variables, by means of the following time or spatial derivatives rules, which are determined by apply chain rule or eulerian time derivative:

$$\nabla_{\underline{X}} f = \underline{J}^{-1} \nabla_{\underline{r}} f \tag{4}$$

$$\frac{df}{dt} = \frac{\partial f}{\partial t} + \nabla_{\underline{X}} f \cdot (\underline{f} - \underline{V}) \tag{5}$$

where f is a generic function on the current configuration, \underline{V} is the velocity vector of the referential points, \underline{J} with $\underline{J} = \nabla_{\underline{r}} \underline{X}$, is the Jacobian of the transformation between spatial and referential configurations.

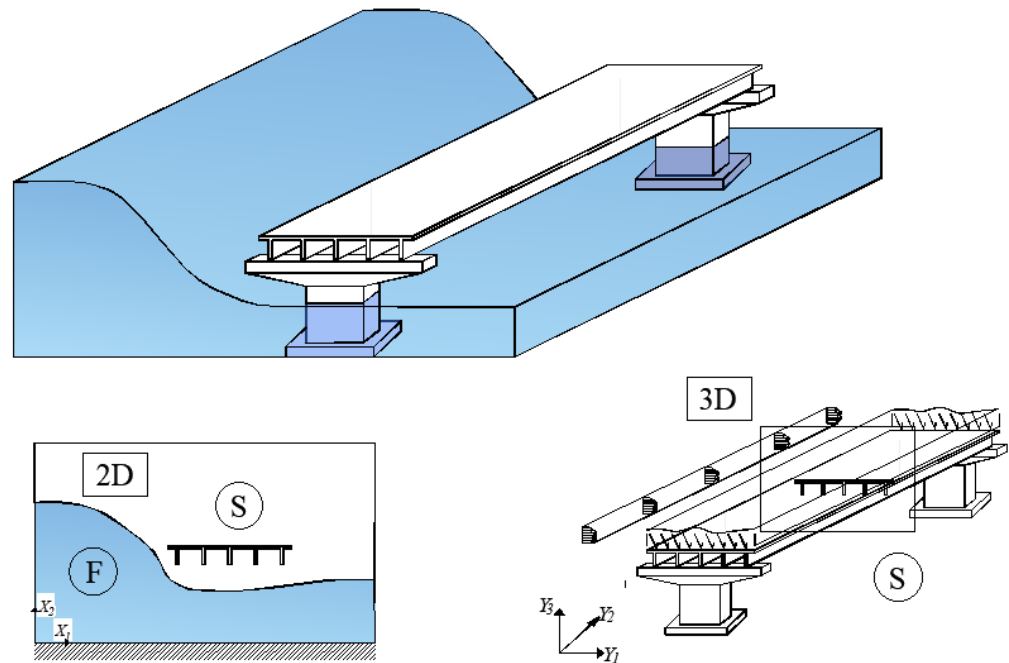


Figure 1. Bridge scheme: fluid (2D) and structural (3D) systems.

In order to reduce mesh distortion during the mesh motion, the ALE formulation requires regularity equations for the positional variables of the computational nodes. This is achieved using a smoothing algorithm based on a “Laplace equation” rezoning method, in which the positions of computational nodes are adjusted by the means of the following expressions, reducing mesh distortions:

$$\nabla_{\underline{r}}^2 X_1 = 0, \nabla_{\underline{r}}^2 X_2 = 0, \quad \text{on } \Xi_0 \tag{6}$$

with X_1 and X_2 representing the horizontal and vertical positions, respectively. Previous equations are completed by boundary and initial conditions, which reproduce the inlet speed flow with fixed on the water depth on Γ_I , zero pressure or wall slip along the external boundaries, i.e., Γ_P and Γ_{SW} respectively. Moreover, moving wall conditions on the fluid/structure interface boundaries, namely Γ_{FSI} , are introduced on the basis of the

structural deformations. In particular, with reference to Figure 1, the following equations are considered:

$$\begin{aligned}
 \underline{U}n &= U_0\Psi(t) && \text{on } \Gamma_I \\
 p &= 0 && \text{on } \Gamma_p \\
 \underline{U}n &= 0 && \text{on } \partial C^{F,w} \\
 U_1(0) &= U_0 && \text{on } C^{F,w}
 \end{aligned}
 \tag{7}$$

where U_0 is the inlet speed and $\Psi(t)$ is the inflow function.

The structural model is based on a continuum solid mechanics formulation, in which classical equations for volume FEs are implemented. In particular, according to ALE formulation, the free surface motion of the solid part in the 2D fluid flow domain is assumed to be equal to the ones of the structural model. Moreover, the structural loads applied on the wall elements affected by the fluid flow should be equal to the pressure distribution arising from the 2D domain. In particular, with reference to Figure 2, the following governing equations are defined:

$$\text{div}\underline{\sigma} + \underline{f} = \underline{I}\mu\underline{\nabla}\underline{\nabla}\cdot\underline{\sigma}, \underline{\sigma} = \underline{E}\underline{\varepsilon}, \underline{\varepsilon} = \underline{\nabla}^s\underline{V},
 \tag{8}$$

where $(\underline{\sigma}, \underline{\varepsilon})$ are the stress and strain tensors, respectively, \underline{E} is the elastic matrix, $\underline{\nabla}^s(\bullet)$ is the symmetric gradient of (\bullet) , and \underline{I} is a 3×3 identity matrix. In addition, boundary conditions are introduced to simulate normal and tangential components of the fluid forces acting on the cross-section contours and prescribed displacements at the bridge ends to take into account the support conditions:

$$\underline{\sigma}n = \underline{f} \text{ on } \partial C_{SW}, \underline{V} = \underline{V}_c \text{ on } \partial\Gamma_{S_V}
 \tag{9}$$

where \underline{f} is the vector containing the forces arising from the fluid flow computation on the external surface of the solid domain, i.e., $[\partial C_{SW} \times L]$, and \underline{V}_c is the vector of prescribed displacements applied at the bridge extremities, namely $\Gamma_{S_V}^c$ (see Figure 3), based on the design bearing scheme.

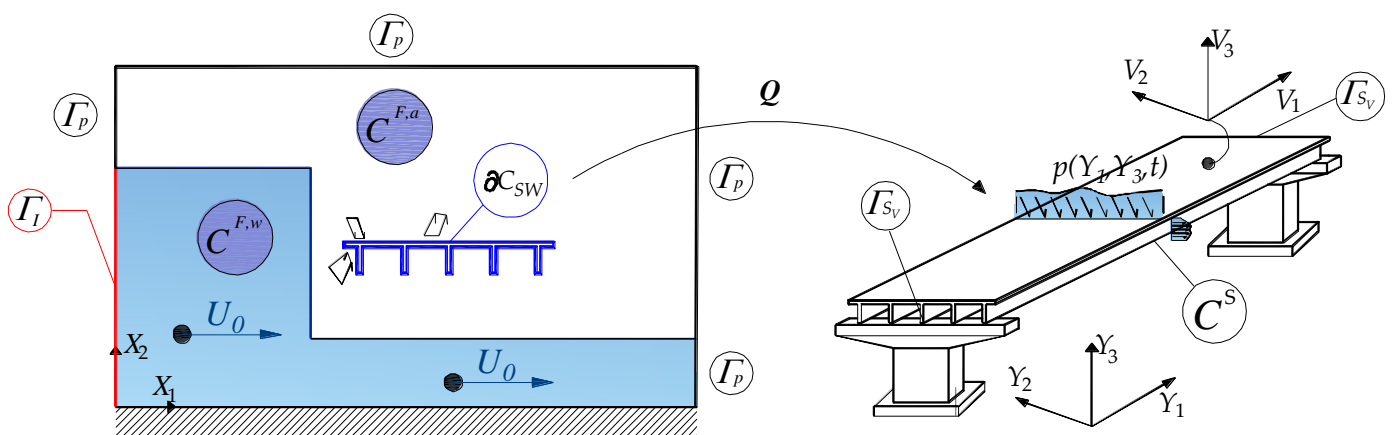


Figure 2. Domains and boundary conditions for the fluid and structure systems.

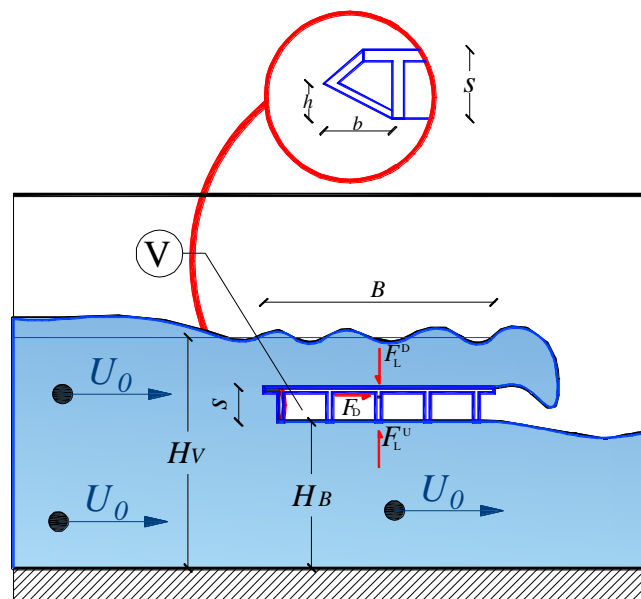


Figure 3. Loading scenarios and inundation parameters. Fairing system configuration.

3. Numerical Implementation

The numerical implementation of the governing equations is developed using a FE approach, based on a customized version of COMSOL MULTIPHYSIC code [24]. The numerical procedure introduces interpolation functions for the fluid and structural problems, i.e., quadratic and cubic, respectively. The discrete equations, obtained by the FE implementation, are solved by an implicit time integration algorithm based on a backward differentiation rule, in which no splitting procedures are adopted. The use of a coupled integration methodology, although it introduces more computational costs, guarantees better accuracy in the solving procedure [25]. For the sake of brevity, the validation is not reported here but details can be recovered in previous authors' works [12,17], in which comparisons with numerical and experimental methods available from the literature are reported. The optimum numerical mesh is chosen by means of sensitivity analyses, in which the characteristic length of the mesh discretization is adopted in such a way to ensure accuracy in the evaluation the fluid and structural variables with relatively low computational costs. In the final computation, the mesh size is controlled by enforcing a maximum length, which is equal, for the investigated cases, to 1 mm. A multi-block analysis with a Delaunay mesh is adopted for all regions with triangular elements, which fit the geometry of each domain better. Moreover, FE boundary layers are adopted at the cross-section lines, in which fluid flow requires more accuracy in view of the turbulence effects.

The loading application is based on a restarting procedure from the initial configuration in which dead and permanent loads are applied. After that, the actions of the fluid flow are considered by performing a time-dependent dynamic analysis. It is worth noting that equations concerning fluid and structural problems are coupled by proper boundary conditions expressed for the geometric entities of both the structural and fluid systems. In particular, the pressure distribution, which corresponds to the applied loads on the structure, depends on the structural displacements by means of the ALE formulation. In contrast, structural deformability is affected by the presence of the applied loads, which are extrapolated on the basis of the pressure distribution on the structure.

The coupling of the variables of both the fluid and structure is defined by a specific mapping function, based on an extrusion methodology implemented in COMSOL, which correspond to one-to-one functions from the 2D to the 3D and vice versa. The trans-

ferring operator is implemented by weak boundary contributions expressed to enforce fluid–structure coupling effects, as follows:

$$\Delta \underline{X} = \underline{Q}^{-1} \underline{V} - \oint_{\partial \Xi^{SW}} \underline{Q} \underline{p} \underline{n} \cdot \delta \underline{V} ds \quad \text{on } \partial C^{SW} \quad (10)$$

where \underline{p} is the vector of surface force on the cross-section boundaries; $\underline{Q} : F \rightarrow S$ and $\underline{Q}^{-1} : S \rightarrow F$ represent the transferring mappings going from the fluid and structural domains and vice versa, $\Delta \underline{X}$ is the vector of the relative positions of the computational nodes and \underline{V} is the displacement vector of the structure at the cross-section boundaries in common with the fluid system.

4. Loading Scheme and Definition of the Fairing System

The results are developed by proper scenarios, which are considered representative of the loading schemes observed during flood or tsunami events. In particular, the effects of incoming wave loads are applied to the structural system, using a water free-surface scheme. Specific characteristics of the impact wave are given in the fluid, namely, the wave height and speed. Such simplified loading schemes are able to reproduce an accurate evaluation of the loading forces on the structure and the FSI effects, involving low computational costs in the numerical model. From the schematic point of view, loading scenarios are represented in Figure 3 [26]. The presence of a fairing system is also investigated, assuming a triangular geometry, attached to the cross-section at the side of the bridge affected by the fluid flow. The loading scenarios are described in terms of non-dimensional parameters, which are representative of the fluid characteristics and bridge properties. In particular, blockage and inundation ratios, Froude number and proximity parameters are defined as follows [27]:

$$B_r = \frac{s}{H_V}, \quad H^* = \frac{H_V - H_B}{s}, \quad P_r = \frac{H_B}{s}, \quad F_r = \frac{U_C}{\sqrt{gH_V}} \quad (11)$$

where s is the thickness of the deck, (H_V, H_B) are the water height and the lower height of the cross-section measured from the ground, respectively, U_C is the flow speed and g is the gravitational constant. The bridge is based on a precast concrete scheme with simply supported boundaries. Such typology is frequently utilized in inland or coastal regions. The analyses are expressed in terms of normalized parameters, which identify geometric, material and inertial properties:

$$L_S = \frac{s}{L}, \quad L_H = \frac{s}{B}, \quad M_r = \frac{E}{MLg}, \quad C_I = \frac{I_{Y_2}}{I_{Y_3}} \quad (12)$$

where M is per unit volume mass, L is the span length, E is Young modulus, I_{Y_2} and I_{Y_3} are inertial moments with respect to transversal and vertical axes, respectively.

5. Results and Discussion

The main aim of the present study is to verify the consistency of formulas typically adopted by existing codes or refined formulations which quantify the effects of tsunamis or flood loads on costal or inland bridges. Such expressions utilize pseudo-static forces in terms of the fluid flow characteristics [28]:

$$\begin{aligned} F_D &= 0.5\rho g(2H_V - 2H_B - s)s + 0.5C_D\rho U_C^2 s \\ F_L^D &= \left[\rho g(H_V - H_B - s)B + 0.5C_{VS}\rho U_C^2 B \right] \\ F_L^U &\approx \left[\rho g(H_V - H_B)B + 0.5C_V\rho U_C^2 B \right] \end{aligned} \quad (13)$$

where C_D is the drag coefficient, (C_{VS}, C_V) are the vertical downward and upward coefficients, respectively, and V is the volume of water displaced by the bridge cross-section. It is worth noting that, in previous formulas, the elevation of free surface is assumed to be constant along the bridge cross-section. Moreover, in Equation (13) the vertical forces are defined by two different contributions related to the Upward (U) or Downward (D) directions, which refer to low or high inundation ratios, respectively. The bridge is based in a simply supported schemes, made of pre-cast concrete in which girder present five main beams. The non-dimensional parameters defined in Equation (12) are:

$$L_S = 0.06, L_H = 0.15, M_r = 40775, C_I = 0.021. \quad (14)$$

In the analysis, the speed and depth of the fluid flow, namely, U_c and H_v , respectively, can be considered as known data, which may be recovered from hydrologic maps developed at the macroscale. In particular, such formulations evaluate representative hydraulic variables, such as speed, water flow distribution and inundation height for specific return periods. However, flood hazard maps at the macroscale only provide the characteristics of the fluid flow, without providing details on the structural response.

The results are developed for loading scenarios with low, moderate or fast flow speeds, measured in terms of the Froude number in the range between 0.5 and 0.75. Moreover, the normalized depths of the flood, measured from the ground level, are assumed to be between 1 and 4. It is worth noting that since elastic behavior is considered for the structural system, the present analyses identify the vulnerability scenarios defined as the distance between the actual status and the one at failure, which is consistent with a stress-based approach. As a consequence, the presented results developed in this framework can be considered as a lower bound prediction with respect to the collapse load level, which requires proper nonlinear models to be used for the structural system. Moreover, dynamic amplification factors are evaluated by comparing the maximum effects observed in a time-dependent dynamic analysis and the corresponding ones assuming the loads applied statically. In order to measure the difference between dynamic and static frameworks, Dynamic Amplification Factors (DAFs) Φ_X , for a generic variable X , are computed as follows [29]:

$$\Phi_X = \frac{\max_{t=0 \dots T} [X]}{X_{ST}} \quad (15)$$

where the subscript ST refers to the value of the X variable obtained by performing a static analysis and T is the observation time. It is worth noting that results in static framework are reproduced by using Equation (13), which are typically utilized in current design procedures for both full or partial inundation phenomena.

The influence of the flow characteristics is investigated in terms of the impact forces applied on the bridge. The time histories of the stress resultant forces applied on the structural system, normalized on the first vertical period of the structure (T_1), are shown in Figure 4. The horizontal drag force increases as the fluid flow application reaches a steady-state flow regime. Moreover, the prediction of the drag force using Equation (13) slightly overestimates the intensity of the hydraulic forces with respect to the dynamic contribution for both values of the inlet fluid flow speed. As a consequence, the use of such formulas leads to safe loading scenarios. For the time histories of uplift forces, the positive values, corresponding to the upward direction, are comparable to the static predictions. As the free water surface reaches the bridge upper chord, the fluid overtops the bridge and negative values with an oscillating trend are observed. The comparisons show that the impact forces evaluated by time-dependent analyses are larger than the values obtained using Equation (13). The time histories of the proposed model are in agreement with several experimental or numerical observations [30], which have shown that an important role in the definition of the upward forces is produced by the air trapped between the girder and free water surfaces. In particular, the *uplift force is the amplified due to the effect of air trapped between the girders.*

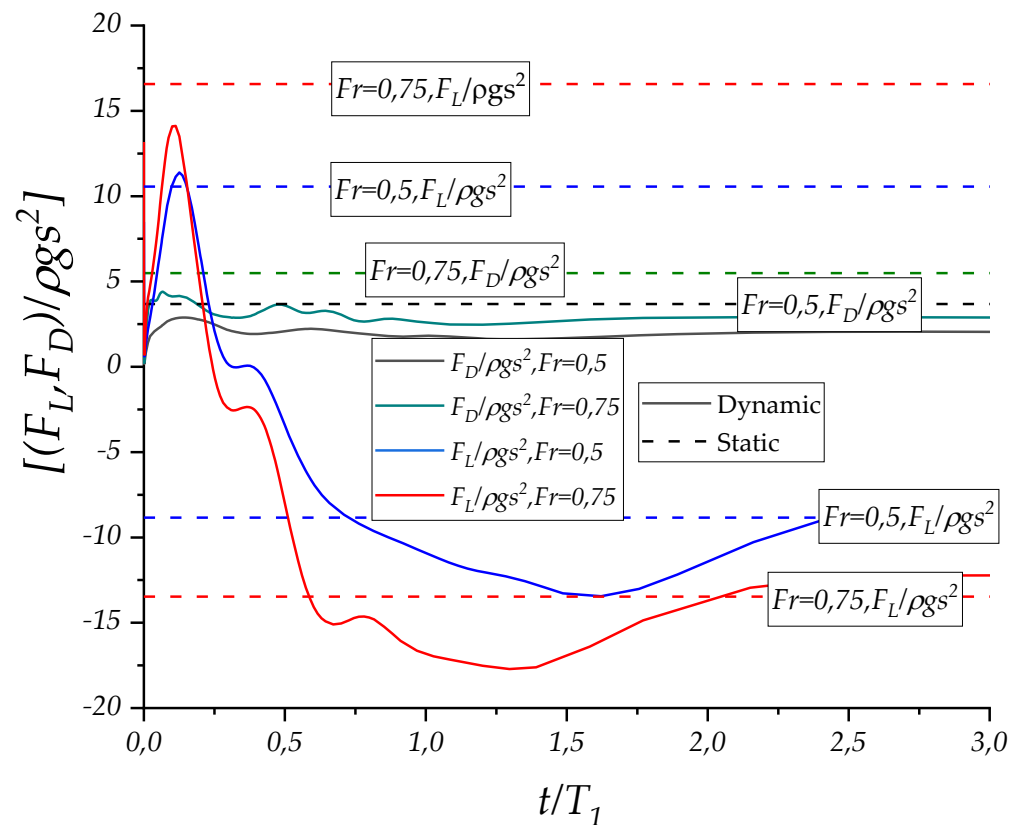


Figure 4. Time histories of normalized drag and lift forces. Comparisons with static values obtained by Equation (13).

The results of dynamic amplification factors are reported in Figure 5. These results are used to analyze the amplification effects produced by the inertial forces on the structure by the action of the fluid flow. The main aim of the proposed results is to quantify the influence of the inertial forces arising from both bridge vibrations or FSI effects. To this end, comparisons with existing formulas provided by a static description of the external loads are carried out. It is worth noting that in static analyses, loading forces are only applied on the structural system, without taking into account the time-dependent effects, which are correctly considered in the dynamic analysis.

Figure 5 illustrates the time histories of the DAFs of the vertical and horizontal displacements at the centroid and extreme side points of the cross-section. In addition, the reaction forces of the bearing system along the horizontal (H) and vertical (V) axes are also reported. Such quantities are quite important, since they are related to the bridge bearing system and thus to the global stability of the structure. As shown in Figure 5, the dynamic amplifications, measured in terms of DAFs, are between 1 and 4.5. The horizontal displacements at both points of the cross-section show large amplifications of the corresponding static values, since the DAFs reach values larger than 2. For vertical displacements, the DAFs reach maximum values equal to 4.5 or -3 , for upward and downward directions, respectively, leading to a general underestimation of the static solution with respect to the actual response. For the reaction forces, similar results are observed for the vertical direction, in which the DAFs are larger than the unity. However, along the horizontal direction, the prediction of the maximum effects is in agreement with the static analysis, since DAFs are close to the unity.

In order to reduce the impacts on the bridge and consequently their effects in terms of displacement or stress fields, several devices are proposed in the literature. A review of tsunami countermeasures is provided in [31]. In the present study, the benefits provided by protection fairing systems applied on the bridge cross-section are investigated. Typically,

they are adopted in long-span bridges or aerospace engineering fields with the aim of avoiding flat boundaries and reproducing airfoil deck cross-sections. From a practical point of view, the installation of such devices can be developed with relative complexities in both new and existing structures, since they are connected at one side of the bridge affected by the fluid flow.

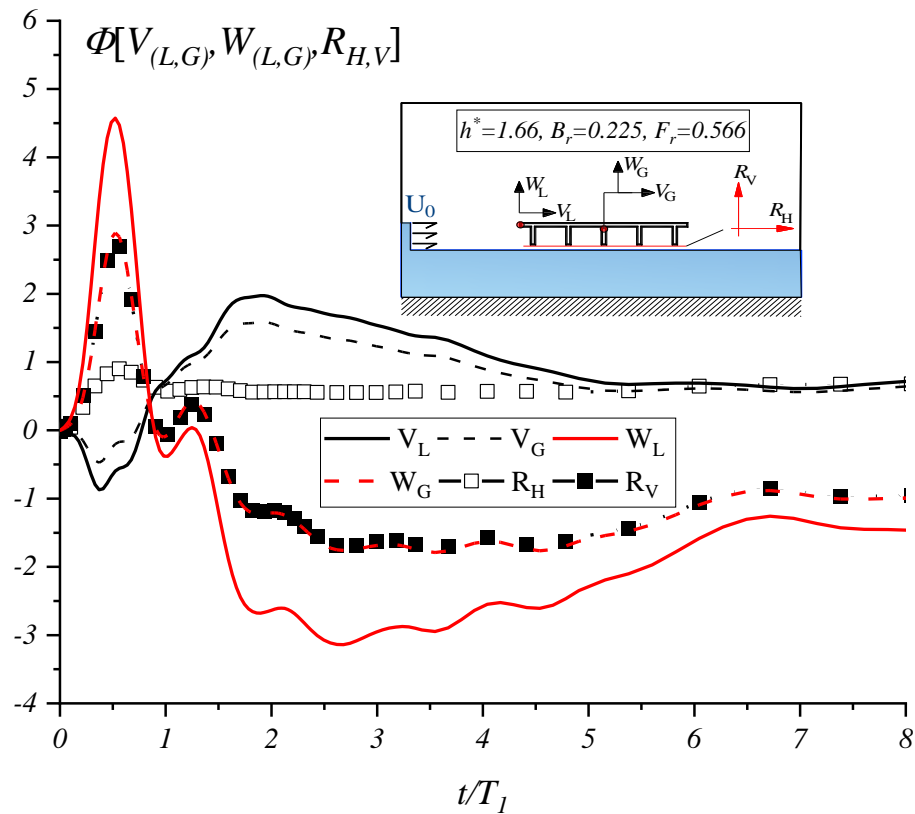


Figure 5. Time histories of the DAFs of the midspan vertical and horizontal displacements at the centroid and the reaction forces of the bearing system.

The shaping effect used to obtain aerodynamic performance is investigated by adopting triangular edges, which can be easily attached at the lower and higher chords of the cross-section. In Figure 3, a schematic view of the deck is illustrated, including the fairing system. In order to verify the efficiency of the fairing system, the following geometry is assumed:

$$b/B = 0.016, h/s = 0.5 \tag{16}$$

The variability of the hydrodynamic drag force in terms of the inundation ratio is presented in Figure 6, in which the maximum values observed during the time histories are reported for the configurations presenting fairing (F) or not protective (NF) fairing systems. The analyses are developed for different normalized flow speeds, expressed using the Froude number. The results show how the drag force increases with the inundation ratio and the Froude number. The comparisons show how the presence of the fairing system can reduce the maximum hydrodynamic forces from impacting the structural system. The analysis of hydrodynamic uplift forces is reported in Figure 7, for both the positive (upward) and negative (downward) directions. The fairing system can reduce both the positive and negative peak values of hydrodynamic forces. The efficiency of the fairing system is also quite important for the large values of the inundations ratios.

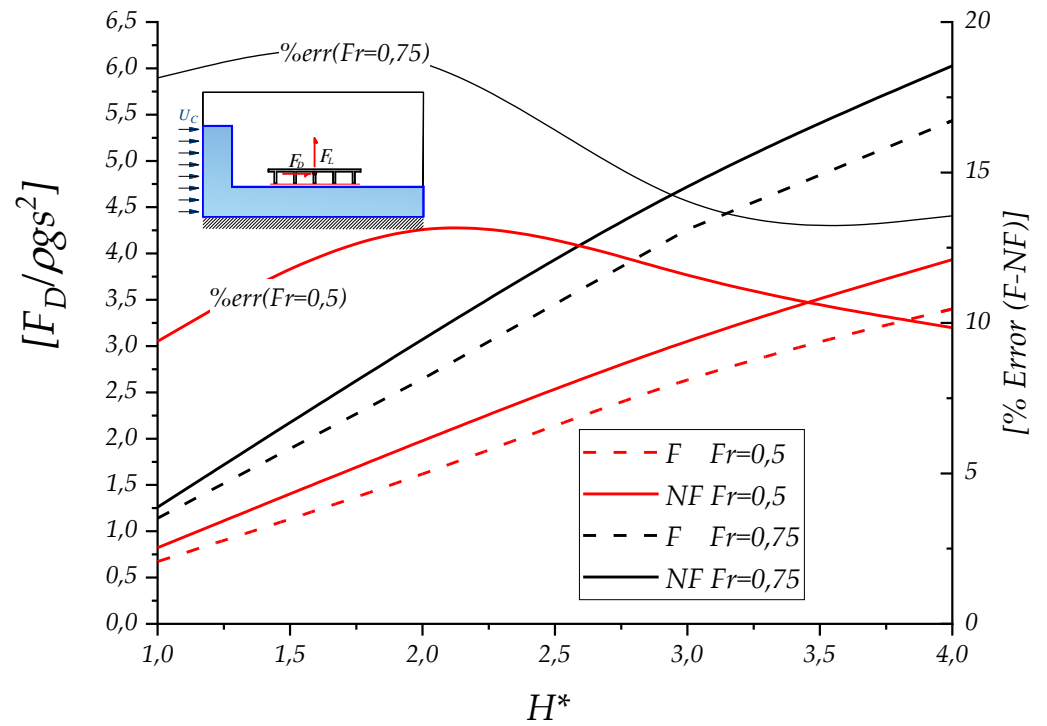


Figure 6. Maximum hydraulic drag force vs. inundation ratio H^* : comparisons between fairing (F) and not fairing (NF) bridge configurations.

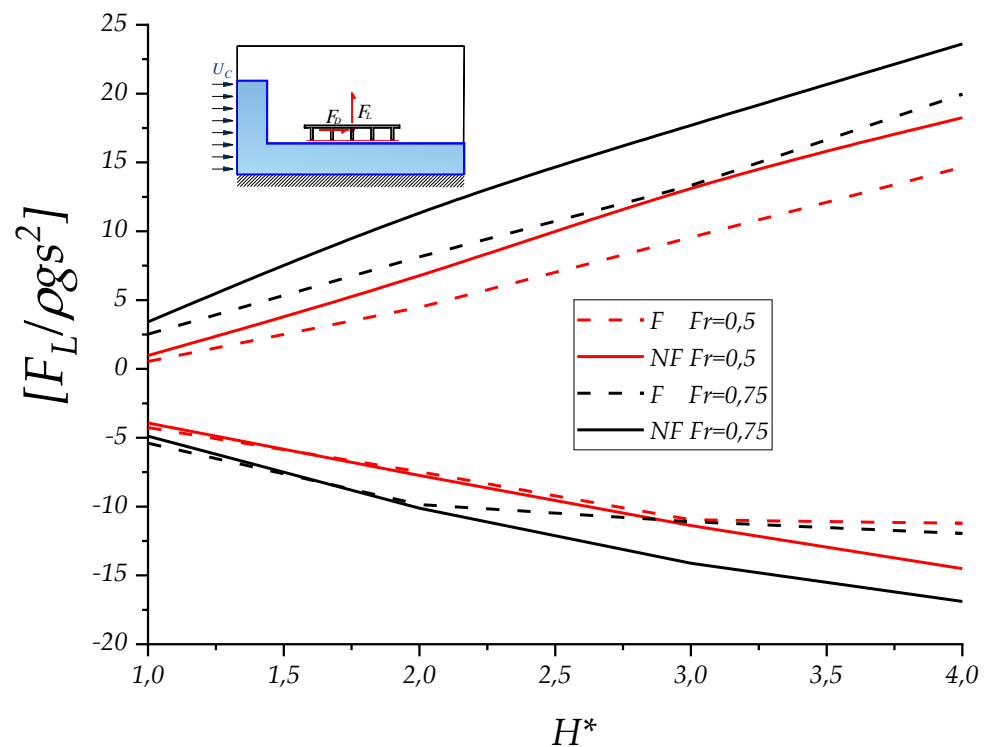


Figure 7. Maximum hydraulic lift force vs. inundation ratio H^* : comparisons between fairing (F) and not fairing (NF) bridge configurations.

The analysis of kinematic quantities is carried out to investigate the effects of the fairing system on bridge deformability. The results, reported in Figures 8 and 9, are expressed in terms of vertical displacements at the centroid axis of the cross-section. The benefits of such a device in terms of the percentage of reductions vary between 15 and 35, depending on

the dimensionless fluid flow speed. In Figure 10, a schematic representation of the phase field fluid is presented for several values of the normalized time, i.e., t/T_1 . The images show how the presence of the fairing system is able to better reduce the impact area of the cross-section, in which the fluid flow acts. Moreover, the pressure distribution is modified by the presence of the fairing system, which is able to reduce the values of the hydrodynamic drag and lift forces.

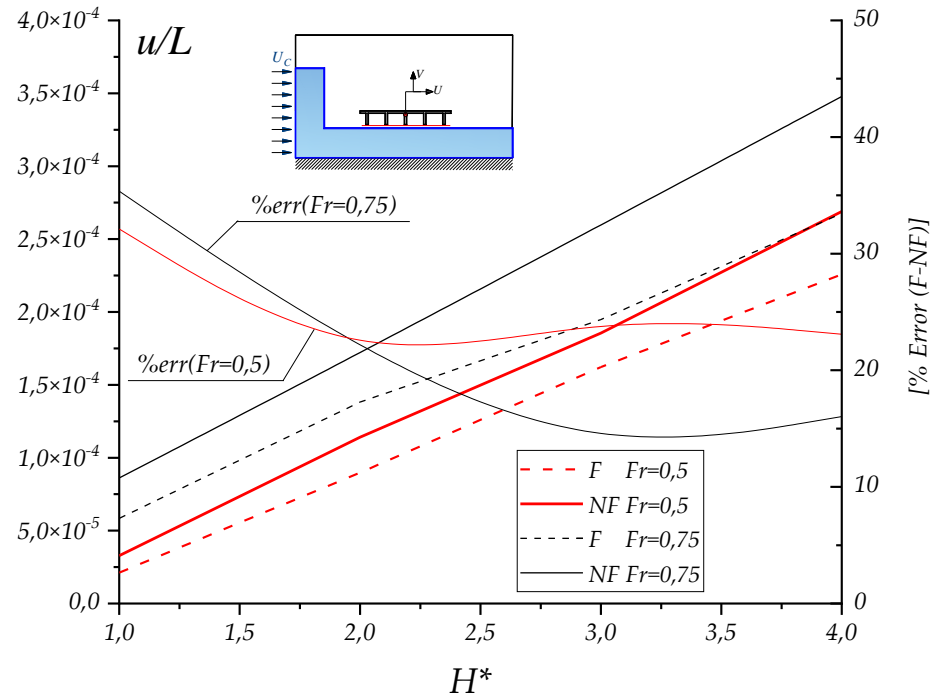


Figure 8. Maximum horizontal bridge displacements vs. inundation ratio H^* : comparisons between fairing (F) and not fairing (NF) bridge configurations.

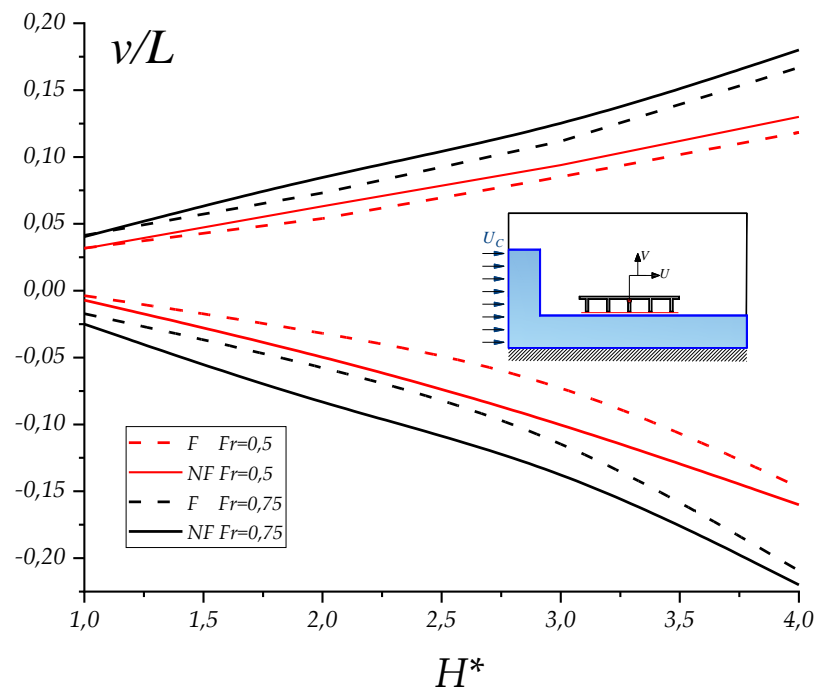


Figure 9. Maximum vertical bridge displacements vs. inundation ratio H^* : comparisons for fairing (F) and not fairing (NF) bridge configurations.

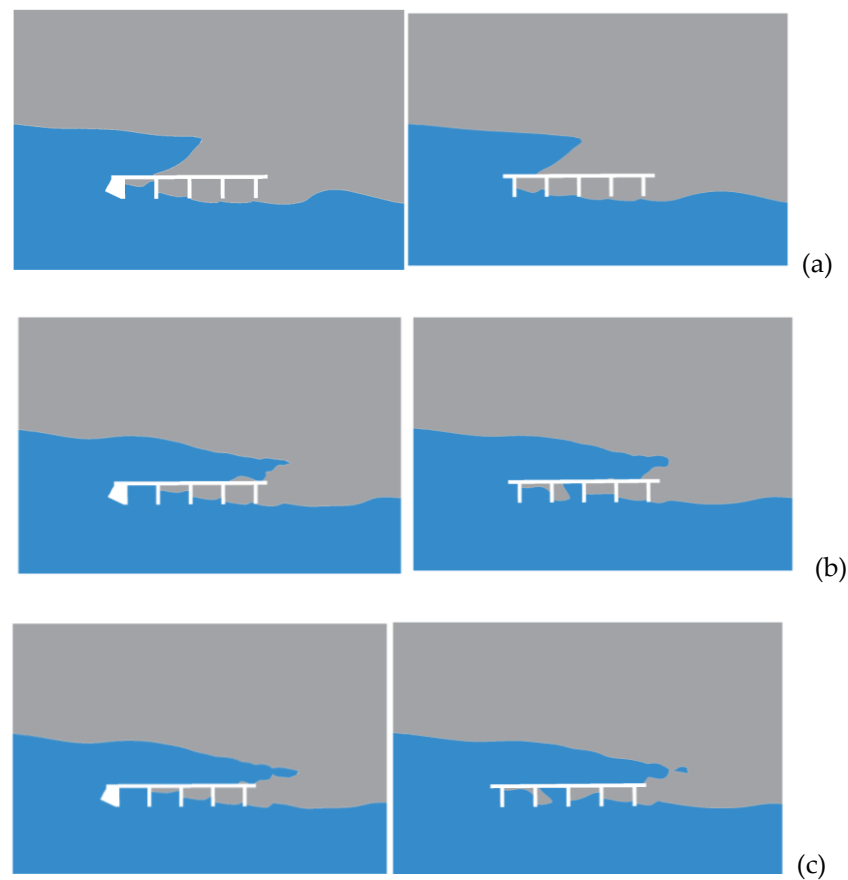


Figure 10. Flow impact at the following times: (a) $t/T1 = 0.35$, (b) $t/T1 = 0.65$ and (c) $t/T1 = 0.72$.

6. Conclusions

The present paper studied the behavior of the fluid–structure interaction of coastal bridges in the presence of extreme floods or tsunami events and investigated the influence of mitigation systems, with the aim of preventing and reducing the damage caused to these structures by the loads. The most relevant scenarios of fluid flow configurations for flood or tsunami events were analyzed using a multiscale model, in which the 2D formulation was based on an ALE-type approach and multiphase fluid flow, whereas a 3D solid mechanics formulation was adopted for the structure. This model can reproduce two-phase fluid flow, bridge deformability and boundary conditions for coupled FSI. Numerical analyses were carried out in terms of dynamic amplification factors (DAF), which proved that existing formulas, available in the literature or in structural design codes, are not accurate in the prediction of maximum design effects. In particular, the evaluation of hydraulic forces or reactions at the bearing system observed in the dynamic analysis may lead to larger values than those estimated using code formulas. Thus, the results of the hydrodynamic forces, bridge displacements and dynamic amplification factors (DAFs) show that the existing formulas cannot accurately predict the maximum design effects. For the investigated cases, the DAFs may vary from 1 to 4.5. The underestimation is quite notable, especially along the vertical direction (upload direction). Sensitivity analyses were also carried out to verify the performance of the protection fairing system. The results show that such devices are able to efficiently reduce the effects of the wave load in terms of the applied hydraulic forces on the structure and bridge deformability. The percentage variation from the unprotected configurations varies between 15 and 35, depending on the dimensionless fluid flow speed.

Author Contributions: Conceptualization, methodology, software, validation, writing—review and editing, F.G. and P.L. All authors have read and agreed to the published version of the manuscript.

Funding: This research received no external funding.

Institutional Review Board Statement: Not applicable.

Informed Consent Statement: Not applicable.

Data Availability Statement: Not applicable.

Conflicts of Interest: The authors declare no conflict of interest.

References

1. Smith, D.I. Flood damage estimation—A review of urban stage-damage curves and loss functions. *Water SA* **1994**, *20*, 231–238.
2. Okeil, A.M.; Cai, C.S. Survey of short-and medium-span bridge damage induced by Hurricane Katrina. *J. Bridge Eng.* **2008**, *13*, 377–387. [[CrossRef](#)]
3. Park, H.; Cox, D.T.; Barbosa, A.R. Probabilistic Tsunami Hazard Assessment (PTHA) for resilience assessment of a coastal community. *Nat. Hazards* **2018**, *94*, 1117–1139. [[CrossRef](#)]
4. Merz, B.; Kreibich, H.; Schwarze, R.; Thieken, A. Review article ‘Assessment of economic flood damage’. *Nat. Hazards Earth Syst. Sci.* **2010**, *10*, 1697–1724. [[CrossRef](#)]
5. Mondoro, A.; Frangopol, D.M. Risk-based cost-benefit analysis for the retrofit of bridges exposed to extreme hydrologic events considering multiple failure modes. *Eng. Struct.* **2018**, *159*, 310–319. [[CrossRef](#)]
6. de Moel, H.; Jongman, B.; Kreibich, H.; Merz, B.; Penning-Rowsell, E.; Ward, P.J. Flood risk assessments at different spatial scales. *Mitig. Adapt. Strateg. Glob. Chang.* **2015**, *20*, 865–890. [[CrossRef](#)]
7. Funari, M.F.; Greco, F.; Lonetti, P. Sandwich panels under interfacial debonding mechanisms. *Compos. Struct.* **2018**, *203*, 310–320. [[CrossRef](#)]
8. Cuomo, G.; Shams, G.; Jonkman, S.; Van Gelder, P. Hydrodynamic loadings of buildings in floods. In *Coastal Engineering 2008*; World Scientific: Singapore, 2009; pp. 3744–3756.
9. Custer, R.; Nishijima, K. Flood vulnerability assessment of residential buildings by explicit damage process modelling. *Nat. Hazards* **2015**, *78*, 461–496. [[CrossRef](#)]
10. Huang, T.Y.; Hsiao, S.C.; Wu, N.J. Nonlinear wave propagation and run-up generated by subaerial landslides modeled using meshless method. *Comput. Mech.* **2014**, *53*, 203–214. [[CrossRef](#)]
11. Xiang, T.; Istrati, D. Assessment of extreme wave impact on coastal decks with different geometries via the arbitrary lagrangian-eulerian method. *J. Mar. Sci. Eng.* **2021**, *9*, 1342. [[CrossRef](#)]
12. Greco, F.; Lonetti, P.; Blasi, P.N. Vulnerability analysis of bridge superstructures under extreme fluid actions. *J. Fluids Struct.* **2020**, *93*, 102843. [[CrossRef](#)]
13. Istrati, D.; Buckle, I.; Lomonaco, P.; Yim, S. Deciphering the Tsunami Wave Impact and Associated Connection Forces in Open-Girder Coastal Bridges. *J. Mar. Sci. Eng.* **2018**, *6*, 148. [[CrossRef](#)]
14. Istrati, D.; Buckle, I. Role of trapped air on the tsunami-induced transient loads and response of coastal bridges. *Geoscience* **2019**, *9*, 191. [[CrossRef](#)]
15. Lonetti, P.; Pascuzzo, A. Design analysis of the optimum configuration of self-anchored cable-stayed suspension bridges. *Struct. Eng. Mech.* **2014**, *51*, 847–866. [[CrossRef](#)]
16. Ross, W. *Damage to Buildings*; Woodhead Publishing: Sawston, UK, 2003.
17. Lonetti, P.; Maletta, R. Dynamic impact analysis of masonry buildings subjected to flood actions. *Eng. Struct.* **2018**, *167*, 445–458. [[CrossRef](#)]
18. Haugen, E.; Kaynia, A. Vulnerability of structures impacted by debris flow. In *Landslides and Engineered Slopes. From the Past to the Future*, 1st ed.; [CD-ROM]; CRC Press: Boca Raton, FL, USA, 2008.
19. Ataei, N.; Padgett, J.E. Limit state capacities for global performance assessment of bridges exposed to hurricane surge and wave. *Struct. Saf.* **2013**, *41*, 73–81. [[CrossRef](#)]
20. Greco, F.; Lonetti, P.; Nevone Blasi, P. Impact mitigation measures for bridges under extreme flood actions. *J. Fluids Struct.* **2021**, *106*, 103381. [[CrossRef](#)]
21. Speziale, C.G. Turbulence modeling for time-dependent RANS and VLES: A review. *AIAA J.* **1998**, *36*, 173–184. [[CrossRef](#)]
22. Donea, J.; Huerta, A.; Ponthot, J.P.; Rodríguez-Ferran, A. *Arbitrary Lagrangian–Eulerian Methods*; John Wiley and Sons: Hoboken, NJ, USA, 2004. [[CrossRef](#)]
23. Funari, M.F.; Lonetti, P. Initiation and evolution of debonding phenomena in layered structures. *Theor. Appl. Fract. Mech.* **2017**, *92*, 133–145. [[CrossRef](#)]
24. COMSOL Multiphysics® Version 5.2. COMSOL AB: Stockholm, Sweden, 2015. Available online: www.comsol.com (accessed on 20 June 2022).
25. Greco, F.; Leonetti, L.; Lonetti, P. A novel approach based on ALE and delamination fracture mechanics for multilayered composite beams. *Compos. Part B Eng.* **2015**, *78*, 447–458. [[CrossRef](#)]
26. Akrişh, G.; Schwartz, R.; Rabinovitch, O.; Agnon, Y. Impact of extreme waves on a vertical wall. *Nat. Hazards* **2016**, *84*, 637–653. [[CrossRef](#)]

27. Azadbakht, M.; Yim, S.C. Simulation and Estimation of Tsunami Loads on Bridge Superstructures. *J. Waterw. Port Coast.* **2015**, *141*. [[CrossRef](#)]
28. Azadbakht, M.; Yim, S.C. Bridge Superstructure Design for Tsunamis: A State-of-the-Art Methodology for Tsunami Modeling, Load Simulation, and Structural Response Assessment. *Struct. Congr.* **2015**, *2015*, 345–354.
29. Chopra, A.K. *Dynamics of Structures: Theory and Applications to Earthquake Engineering*; Pearson/Prentice Hall: Hoboken, NJ, USA, 2007.
30. Araki, S.; Deguchi, I. Experimental Study on Tsunami Fluid Force on Bridge across Narrow River. In *Asian and Pacific Coasts 2009*; World Scientific: Singapore, 2010; pp. 143–150.
31. Oetjen, J.; Sundar, V.; Venkatachalam, S.; Reicherter, K.; Engel, M.; Schüttrumpf, H.; Sannasiraj, S.A. A comprehensive review on structural tsunami countermeasures. *Nat. Hazards* **2022**. [[CrossRef](#)]